Received: 29 December 2021 | Revised: 9 June 2022 | Accepted: 18 June 2022

DOI: 10.1002/jcla.24578

RESEARCH ARTICLE

WILEY

Rapid detection of the irinotecan-related *UGT1A1**28 polymorphism by asymmetric PCR melting curve analysis using one fluorescent probe

Xiaomu Kong[1] | Ye Xu[2] | Peng Gao[1] | Yi Liu[1] | Xuran Wang[2] | Meimei Zhao[1] | Yongwei Jiang[1] | Hui Yang[1] | Yongtong Cao[1] | Liang Ma[1]

[1]Department of Clinical Laboratory, China-Japan Friendship Hospital, Beijing, China

[2]Engineering Research Centre of Molecular Diagnostics, Ministry of Education, State Key Laboratory of Cellular Stress Biology, School of Life Sciences, Xiamen University, Xiamen, China

Correspondence
Liang Ma and Yongtong Cao, Department of Clinical Laboratory, China-Japan Friendship Hospital, No. 2 Yinghua East Street, Chaoyang District, Beijing 100029 China.
Emails: liangma321@163.com (L.M.); caoyongtong92@sina.com (Y.C.)

Funding information
This work was supported by the National Natural Science Foundation of China (grant number 81200536, 82074221 and 82072337), Key Clinical Specialty Project of Beijing (grant number 2020), and Elite Medical Professionals project of China-Japan Friendship Hospital (grant number ZRJY2021-GG03). The funders had no role in study design, data collection and analysis, decision to publish, or preparation of the manuscript.

Abstract

Background: Determination of *UGT1A1* $(TA)_n$ polymorphism prior to irinotecan therapy is necessary to avoid severe adverse drug effects. Thus, accurate and reliable genotyping methods for $(TA)_n$ polymorphism are highly desired. Here, we present a new method for polymerase chain reaction (PCR) melting curve analysis using one fluorescent probe to discriminate the *UGT1A1**1 [$(TA)_6$] and *28 [$(TA)_7$] genotypes.

Methods: After protocol optimization, this technique was applied for genotyping of 64 patients (including 23 with *UGT1A1**1/*1, 22 with *1/*28, and 19 with *28/*28) recruited between 2016 and 2021 in China-Japan Friendship Hospital. The accuracy of the method was evaluated by comparing the results with those of direct sequencing and fragment analysis. The intra- and inter-run precision of the melting temperatures (T_ms) were calculated to assess the reliability, and the limit of detection was examined to assess the sensitivity.

Results: All genotypes were correctly identified with the new method, and its accuracy was higher than that of fragment analysis. The intra- and inter-run coefficients of variation for the T_ms were both ≤0.27%, with standard deviations ≤0.14°C. The limit of detection was 0.2 ng of input genomic DNA.

Conclusion: The developed PCR melting curve analysis using one fluorescent probe can provide accurate, reliable, rapid, simple, and low-cost detection of *UGT1A1* $(TA)_n$ polymorphism, and its use can be easily generalized in clinical laboratories with a fluorescent PCR platform.

KEYWORDS
genetic testing, irinotecan, melting curve analysis, pharmacogenetics, *UGT1A1*

Xiaomu Kong and Ye Xu contributed equally to the present work.

1 | INTRODUCTION

Glucuronidation, which is catalyzed by the UDP-glucuronosyltransferases (UGTs), has an essential role in the metabolism of xenobiotic and lipophilic endobiotic substrates, such as bilirubin and the chemotherapeutic drug irinotecan.[1] UGT1A1, belonging to the UGT1A subfamily, is responsible for hepatic glucuronidation of bilirubin. The *UGT1A1* gene is located on chromosome 2q37. Multiple variations in the *UGT1A1* gene can alter the enzyme activity of UGT1A1 protein.[2–4] Among them, the promotor $(TA)_n$ polymorphism (rs3064744) is one of the most frequently investigated. Its wild-type sequence contains six repeats of TA [$(TA)_6$, *UGT1A1**1], whereas the other alleles contain either five TA repeats [$(TA)_5$, *UGT1A1**36] with normal or increased *UGT1A1* expression or seven [$(TA)_7$, *UGT1A1**28] and eight TA repeats [$(TA)_8$, *UGT1A1**37] with decreased *UGT1A1* expression and thus a reduction of its enzyme activity.[2,3,5] *UGT1A1**28 is the most common $(TA)_n$ variant, with reported allelic frequencies of 29%–45% in Caucasians, 42%–51% in Africans, and 16% in Asians.[6] The *UGT1A1**36 and *37 variants occur almost exclusively in Africans.[7,8]

Decreased UGT1A1 enzyme activity leads to disordered glucuronidation, resulting in defects in bilirubin metabolism. Individuals who are homozygous or compound heterozygous for the *UGT1A1**28 and *37 alleles develop the inherited Gilbert's syndrome (OMIM 143500) characterized by mild unconjugated hyperbilirubinemia, which is commonly a benign condition, and a more aggressive childhood subtype, Crigler-Najjar syndrome (OMIM 218800, 606785).[6,9]

More importantly, extensive studies indicate that *UGT1A1**28 carriers (homozygotes and heterozygotes) have a significantly higher risk for life-threatening, adverse effects from irinotecan treatment in multiple races and populations.[6,10–14] Irinotecan, a camptothecin analog, is a chemotherapeutic drug widely used in the treatment of metastatic colorectal cancer (first-line treatment) and occasionally used for treating other solid tumors.[15] A significant proportion of patients taking irinotecan experience life-threatening adverse effects including leukopenia, neutropenia, and/or diarrhea, due to the reduced elimination of SN-38 (7-ethyl-10-hydroxycamptothecin), the active metabolite of irinotecan, which is primarily glucuronidated by hepatic UGT1A1 protein.[4,6,16] A meta-analysis based on 58 studies including 6087 cancer patients showed that individuals carrying *UGT1A1**1/*28 and *28/*28 have a greater prevalence of diarrhea and neutropenia than those carrying *UGT1A1**1/*1 with odds ratios of 2.18 and 2.15, respectively, specifically for patients with metastatic colorectal cancer.[17] In 2005, the Food and Drug Administration (FDA) added the genetic status of $(TA)_n$ polymorphism to the drug label for irinotecan, recommending that patients with a *UGT1A1**28/*28 genotype should receive a lower starting dose of irinotecan. Moreover, the results from an updated meta-analysis conducted in 2010 involving 1998 cancer patients indicate that the *UGT1A1**28/*28 genotype is associated with a 2-fold increased risk of neutropenia not only at medium doses but also at low doses.[16] Thus, there is an urgent need to develop rapid and accurate genotyping methods for $(TA)_n$ polymorphism. If the $(TA)_n$ genotype is determined prior to the therapy initiation, the occurrence of the adverse reactions to irinotecan could be prevented.

To date, multiple assays have been applied in attempts to facilitate precision irinotecan therapy, including denaturing gradient gel electrophoresis,[18] dual hybridization probe melting analysis,[19–22] SYBR Green I melting analysis,[23] a single-strand conformation polymorphism (SSCP) method,[24] pyrosequencing,[25–27] the FDA-approved Invader® assay,[28] fragment analysis,[29–31] hydrolysis probes,[32,33] high-resolution melting (HRM) curve analysis,[34,35] a denaturing high-performance liquid chromatography (DHPLC) method,[36] a microarray with LNA-probes,[37] a restriction fragment length polymorphism (RFLP) method,[38] and a three-dimensional polyacrylamide gel-based DNA microarray.[39] Two studies have compared these established genotyping methods. Baudhuin et al.[40] compared the direct sequencing, fragment analysis, and Invader® assay methods. They found that although all samples had concordant genotypes, the interpretation of sequencing data was challenging, and the Invader® assay required more concentrated DNA and was more expensive. In 2020, Sissung et al.[41] compared eight $(TA)_n$ polymorphism genotyping technologies (i.e., direct sequencing, pyrosequencing, gel sizing, DMET Plus arrays, Pharmacoscan arrays, Illumina MiSeq, fragment analysis, and fluorescent PCR), and from their results, they recommended that all genotyping be conducted with fluorescent PCR, as the results from the other platforms were often ambiguous or incorrect. They also suggested that a novel methodology based on fluorescent PCR will be a promising direction for the development of an accurate and reliable genotyping platform for $(TA)_n$ polymorphism that can easily be generalized.

In the present study, we developed a novel method for *UGT1A1**1/*1, *1/*28, and *28/*28 genotyping based on asymmetric PCR and melting curve analysis with one fluorescent probe and demonstrated that this method is accurate, stable, rapid, and simple with cost-efficient performance.

2 | MATERIALS AND METHODS

2.1 | Patients

Sixty-four participants, who previously underwent *UGT1A1* $(TA)_n$ promoter polymorphism genotyping by fragment analysis, were recruited between 2016 and 2021 in China-Japan Friendship Hospital. Written informed consent was obtained for all participants. The study protocol was developed in accordance with the Declaration of Helsinki II and approved by the ethics committee of the hospital. Two-milliliters of whole blood samples from all participants were collected into EDTA-anticoagulated tubes and stored at 4°C before DNA extraction. The clinical characteristics of the participants are presented in Table S1.

2.2 | DNA sample preparation

Genomic DNA was extracted using a DNA extraction kit (Tianlong Science and Technology Co. Ltd) according to the manufacturer's instruction. The DNA was dissolved in TE buffer (10 mmol/L Tris and 0.1 mmol/L EDTA, pH 8.0) to 30–60 ng/μl as measured at 260 nm by a NanoDrop 1000 (Thermo Fisher Scientific) and then stored at −20°C. For sensitive analyses, DNA was diluted to 0.1–0.2 ng/μl using nuclease-free water (Ambion, Life Technologies Corp).

2.3 | Plasmid construction

Plasmids with *UGT1A1* $(TA)_n$ promoter genotypes *UGT1A1**1 and *28 were obtained from Sangon Biotech Co., Ltd. In brief, a fragment containing the *UGT1A1**1 or *28 polymorphism was inserted into the plasmid pUC57. The insert sequences of plasmids are presented in Table S2. The heterozygote of *UGT1A1**1 and *28 alleles was constructed by mixing the plasmids equally.

2.4 | Fragment analysis using capillary electrophoresis

The initial genotyping of *UGT1A1* $(TA)_n$ promoter polymorphisms was achieved using PCR amplification and fragment analysis. The sequences of PCR primer pairs were designed as follows: 5'–FAM-CTCC CTGCTACCTTTGTGGACTGA–3′ (forward primer; FAM is a fluorescent dye with emission at 518 nm and excitation at 492 nm; TaKaRa Bio, Inc.), 5'–ACAACGAGGCGTCAGGTGCTA–3′ (reverse primer; TaKaRa Bio Inc.). PCR was carried out in a 10-μl reaction volume containing 30–60 ng of genomic DNA and GoTaq® DNA Polymerase supplied in 2 × GoTaq® Green Reaction Buffer (pH 8.5), dNTP (400 μM each) and 3 mM $MgCl_2$ (M7122: Promega), with 0.4 μM of each primer. The PCR cycling program consisted of initial denaturation at 94°C for 5 min followed by 40 cycles of 94°C for 15 s, 55°C for 25 s, and 72°C for 50 s, and a final extension at 72°C for 10 min was performed (C1000: Touch™ Thermal Cycler, Bio-Rad Laboratories, Inc.). The amplified product for *UGT1A1**1 was 339 bp, and that for *UGT1A1**28 was 341 bp.

The amplicons were diluted 1:20 with nuclease-free water (Ambion, Life Technologies Corp.). Then, 1 μl of the diluted DNA was mixed with 9 μl Hi-Di™ formamide (Applied Biosystems) and 1 μl genescan™ 500 LIZ® Size Standard (Applied Biosystems). The mixtures were denatured at 95°C for 5 min using a C1000 Touch™ Thermal Cycler (Bio-Rad Laboratories, Inc.) and then quenched on ice. Samples were separated by capillary electrophoresis on the ABI 3500 Genetic Analyzer (Applied Biosystems) using POP-7™ Performance Optimized Polymer (Applied Biosystems) and a 50-cm capillary array following the parameters below: 60°C run temperature, 15 kV pre-run voltage for 180 s, 1.6 kV injection voltage for 8 s, and a 19.5 kV run voltage for 1330 s with a 1-s data delay. Sample migration distances were analyzed using genemapper® Software (Applied Biosystems) to determine the genotype.

2.5 | Asymmetric PCR and melting curve analysis with one fluorescent probe

The PCR primers were designed as follows: 5'–TGAACTCCCTGCTACCTTTG–3′ (forward primer; Sangon Biotech Co., Ltd.), and 5'–CAACAGTATCTTCCCAGCAT–3′ (reverse primer; Sangon Biotech Co., Ltd.). The fluorescent probe used to detect $(TA)_n$ polymorphism was designed as 5'–BHQ2-GCCATATATATATATATAAG TAGG-Cy5–3′ (BHQ2 is a quencher dye; Cy5 is a fluorescent dye with emission at 670 nm and excitation at 649 nm; Sangon Biotech Co., Ltd.).

For PCR, different concentrations of Mg^{2+} (1, 2, 3, 4, and 5 nM) as well as different proportions of forward and reverse primers (forward primer: reverse primer = 2:1, 1:1, 1:2, 1:4, 1:8, 1:16) were tested to optimize the protocol. Finally, PCR was carried out in a 25-μl optimized reaction mixture containing 150–300 ng of genomic DNA and TaKaRa Ex Taq® Polymerase (0.125 U) supplied in 10 × Ex Taq Buffer (pH 8.5), dNTP (200 μM each), and 2 mM $MgCl_2$ (RR01AM, TaKaRa Bio, Inc.), with 0.1 μM forward primer, 0.8 μM reverse primer, and 0.4 μM probe.

The PCR amplification and melting curve analysis were performed on a slan®-96P fluorescent quantitative PCR system (Hongshitech). The PCR cycling program consisted of initial denaturation at 95°C for 5 min followed by 50 cycles of 95°C for 20 s and 60°C for 1 min for amplification. The amplified products for *UGT1A1**1 and *28 were 240 bp and 242 bp, respectively. The melting curve program included three steps: denaturation at 95°C for 2 min, renaturation at 45°C for 2 min, and subsequent melting with continuous acquisition of fluorescence from 45 to 75°C at a ramp rate of 0.08°C/s.

The analytical sensitivity of the present method was evaluated by examining its performance with varying amounts of input genomic DNA used for PCR. We selected two samples of each genotype with an initial concentration ranging from 31.9 to 40.5 ng/μl, and prepared doubling dilutions 11 times to a lowest concentration ranging from 0.016 to 0.020 ng/μl (Table S3). Thus, an input DNA amount as low as 0.1 ng was used to test the limit of detection.

2.6 | Sanger sequencing

The genotype of each patient was confirmed by Sanger sequencing. PCR was performed as described for fragment analysis except that the forward primer was not fluorescently labeled, and the reaction volume was 50 μl, containing 150–300 ng of genomic DNA. The amplicons were then sent to Tsingke Biotechnology Co., Ltd. for unidirectional sequencing using an ABI 3730xl DNA Analyzer (Applied Biosystems).

2.7 | Statistics

The data are presented as mean ± standard deviation (SD), and the coefficients of variation (CVs) were calculated using sas (version 9.3; SAS Institute).

3 | RESULTS

3.1 | Protocol optimization

To optimize the protocol for the new melting curve method, different concentrations of Mg^{2+} (1, 2, 3, 4, and 5 nM) as well as different proportions of forward and reverse primers (F: R = 2:1, 1:1, 1:2, 1:4, 1:8, 1:16) in the PCR reaction mixture, were tested. As shown in Figures S1 and S2, 2 nM of Mg^{2+} and an F:R ratio of 1:8 were finally chosen as the optimized conditions for subsequent analyses.

3.2 | Accuracy

We used three methods for genotyping the $(TA)_n$ polymorphism in 64 patients (Figure 1). Using Sanger sequencing as the gold standard for genotyping, DNA samples were first genotyped via a reference method, fragment analysis using capillary electrophoresis. The genotypes of the 64 patients included *UGT1A1**1/*1 in 23 patients, *1/*28 in 22 patients, and *28/*28 in 19 patients. The melting curve approach was then performed blindly with fragment analysis. The accuracy of this melting curve analysis was validated and compared with fragment analysis. Among the samples, the results of melting curve analysis reached 100% concordance with Sanger sequencing in all genotypes. The fragment analysis showed 100% concordance with Sanger sequencing for *UGT1A1**1/*1 and *1/*28 samples. However, for *UGT1A1**28/*28, when applying fragment analysis, two of the 19 *28/*28 individuals were misclassified as *1/*28, resulting in 89.47% concordance with Sanger sequencing (Table 1). These results indicated that the melting curve analysis offered a higher accuracy than fragment analysis.

The melting temperatures (T_ms) of the *UGT1A1**1 peak in *1/*1 and *1/*28 samples were 56.50 ± 0.09°C and 56.67 ± 0.08°C, respectively. For the *UGT1A1**28 peak, the T_ms in *28/*28 and *1/*28 samples was 52.28 ± 0.09°C and 52.07 ± 0.09°C, respectively.

The melting curve analysis was also validated by analysis of three replicates of each genotype using plasmids (Figure S3). The T_ms of the *UGT1A1**1 peak for the *1 plasmid and mixture of *1 and *28 plasmids were 56.29 ± 0.05°C and 56.66 ± 0.02°C, respectively. The T_ms of the *UGT1A1**28 peak in the *28 plasmid and mixture of *1 and *28 plasmids were 52.30 ± 0.03°C and 52.10 ± 0.03°C, respectively.

3.3 | Precision

We evaluated the diagnostic reliability of the newly developed method. Five replicates of one sample of each genotype were tested on four independent days by different operators to determine the intra-run and inter-run precision. As shown in Table 2, we obtained an intra-run T_m CV ≤ 0.27% (ranging from 0.03% to 0.27%) with an SD ≤ 0.14°C (ranging from 0.02 to 0.14°C) and an inter-run T_m CV ≤ 0.27% (ranging from 0.17% to 0.27%) with an SD ≤ 0.14°C (ranging from 0.09 to 0.14°C). The melting curves also showed good reproducibility (Figure S4).

3.4 | Limit of detection

To evaluate the limit of detection for the melting curve method, we diluted two samples of each genotype to an input DNA amount of 0.1 ng (Table S3). The present method could detect each genotype correctly with a sensitivity as low as 0.2 ng (Figure S5).

4 | DISCUSSION

Genotyping of the *UGT1A1* $(TA)_n$ promoter polymorphism prior to irinotecan therapy is of great importance to minimizing the risk of severe adverse drug effects linked to the *UGT1A1**28 variant, which can cause reduced gene transcription and deficient UGT1A1 enzyme activity. Clinical trials have suggested that irinotecan therapy guided by *UGT1A1* status can significantly increase the likelihood of complete tumor response[42] and achieve a favorable clinical outcome without significantly increased toxicities.[43–46] The FDA has already recommended a reduced initial dose of irinotecan for patients carrying the *UGT1A1**28 variant. Therefore, an accurate, rapid, simple, and reliable genotyping assay for the $(TA)_n$ polymorphism, especially for the *UGT1A1**1 and *28 alleles, is required urgently.

The gold standard method for *UGT1A1* $(TA)_n$ promoter genotyping is direct Sanger sequencing, but it is laborious, time-consuming, and expensive. Fragment analysis by capillary electrophoresis is frequently used,[29–31] but the operating procedure is complicated and also time-consuming. Additionally, fragment analysis unavoidably returns a range of fragment sizes [stutter (*n*–1) repeats shorter than the allele] in addition to the targeted fragment due to Taq polymerase "slippage", which might cause operator bias when discriminating genotypes, especially among inexperienced operators.[29,31,47] In the present study, the recruited patients were initially genotyped using fragment analysis, and two *UGT1A1**28/*28 samples were misclassified as *1/*28, due to misjudgment of stutter peaks by the operators. In addition, for *UGT1A1**1/*28 heterozygotes, the amplification of the *1 allele was stronger than that of *28 allele, and thus, the judgment of the *28 peak might be subjectively influenced by the operator. Moreover, both methods require transfer of the PCR amplification products, which could induce laboratory contamination. A DNA sequencing platform is required for both techniques, which is expensive and may not be available in some clinical laboratories. These platforms also require routine, time-consuming, and labor-intensive maintenance. In fact, in China for example, although direct sequencing and fragment analysis are the only two methods approved by the National Medical Products Administration of China (also known as CFDA) for *UGT1A1* $(TA)_n$ promoter polymorphism genotyping, a gene sequencer is not available in most clinical laboratories. Thus, the testing cannot be performed locally, and the results are therefore delayed for patients.

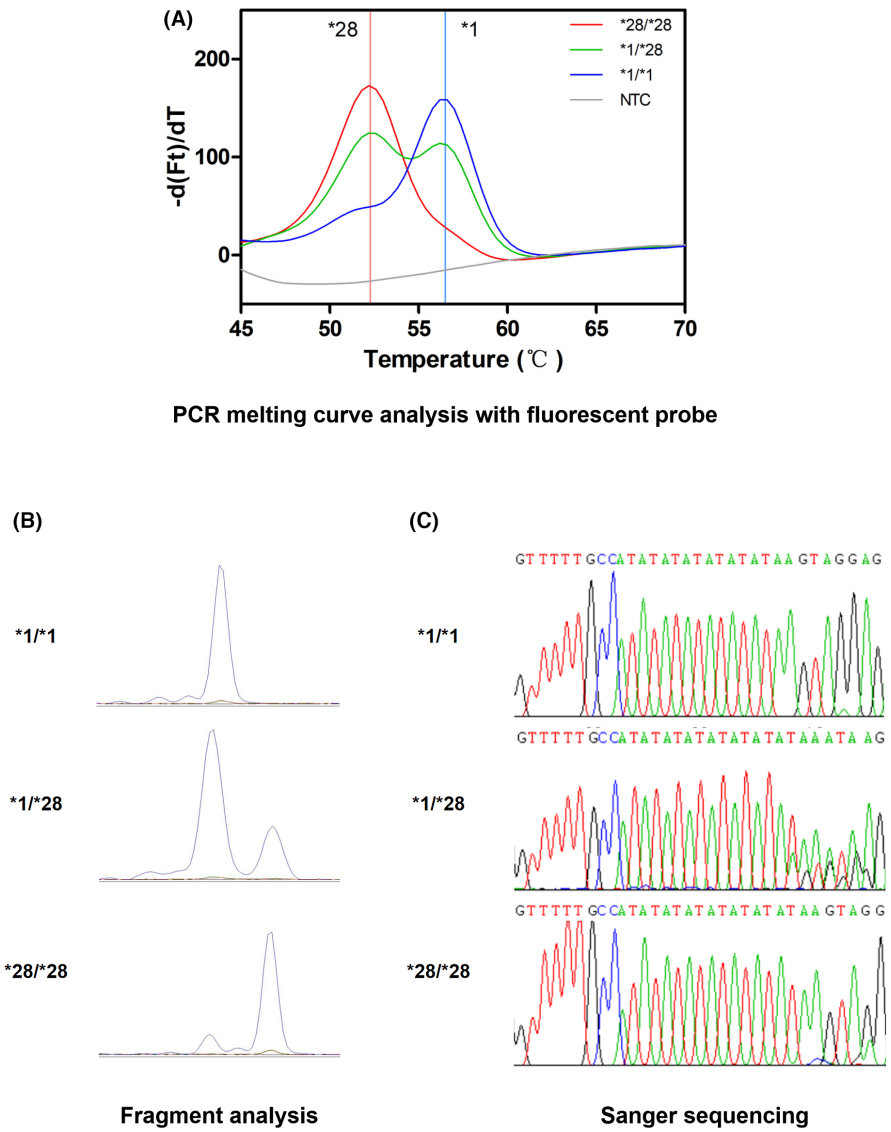

FIGURE 1 Representative melting curve and electropherograms for *UGT1A1**1/*1, *1/*28, and *28/*28 genotypes in patients. (A) Melting curve analysis with one fluorescent probe. (B) Fragment analysis. (C) Sanger sequencing

TABLE 1 Accuracy comparison of PCR melting curve analysis versus fragment analysis for *UGT1A1**1/*1, *1/*28, and *28/*28 genotyping

		Fragment analysis		PCR melting curve analysis using fluorescent probe	
Sanger sequencing genotype	*N*	$N_{Correct}/N_{Total}$	Concordance, %	$N_{Correct}/N_{Total}$	Concordance, %
*UGT1A1**1/*1	23	23/23	100	23/23	100
*UGT1A1**1/*28	22	22/22	100	22/22	100
*UGT1A1**28/*28	19	17/19	89.47	19/19	100

Melting curve analysis based on fluorescent PCR has been adapted for $(TA)_n$ polymorphism genotyping. Among the established methodologies, a melting curve with dual hybridization fluorescent probes has been most frequently reported.[19–22] These approaches are accurate and offer good reliability. However, they require at least two probes for the discrimination of *UGT1A1**1/*1, *1/*28, and *28/*28 genotypes. Dye-based melting curve analyses have also been applied, which only require intercalation dyes of double-stranded DNA. A method based on SYBR Green I showed a T_m difference of only 1.3°C between the 132-bp products of *UGT1A1**1 homozygotes and the 134-bp products of *28 homozygotes, which resulted in limited resolution and difficultly identifying the difference.[23] An HRM approach based on LC-Green was reported to successfully distinguish *UGT1A1**1/*1, *1/*28, and *28/*28 genotypes from a 70-bp product with LC-Green.[34] Another technology based on PCR using a snapback primer and genotyping by HRM was able to discriminate the other two rare genotypes.[35] However, generating reproducible melting curves is always a challenge for HRM analysis, which requires high-resolution instrumentation and targeted software. Moreover, dyes cannot distinguish the target amplicons

TABLE 2 Inter- and intra-run mean ± SDs precision values of T_ms for *UGT1A1**1/*1, *1/*28 and *28/*28

		*UGT1A1**1 peak				*UGT1A1**28 peak			
		Intra-run T_m		Inter-run T_m		Intra-run T_m		Inter-run T_m	
Genotype	Day	Mean ± SD, °C	CV (%)	Mean ± SD, °C	CV (%)	Mean ± SD, °C	CV (%)	Mean ± SD, °C	CV (%)
*UGT1A1**1/*1	1	56.47 ± 0.04	0.06	56.41 ± 0.09	0.17	/	/	/	/
	2	56.40 ± 0.03	0.05			/	/		
	3	56.48 ± 0.08	0.14			/	/		
	4	56.28 ± 0.06	0.10			/	/		
*UGT1A1**1/*28	1	56.62 ± 0.12	0.22	56.66 ± 0.13	0.23	52.05 ± 0.14	0.27	52.06 ± 0.14	0.27
	2	56.68 ± 0.02	0.03			52.11 ± 0.03	0.05		
	3	56.82 ± 0.03	0.06			52.20 ± 0.03	0.06		
	4	56.52 ± 0.08	0.14			51.89 ± 0.10	0.18		
*UGT1A1**28/*28	1	/	/	/	/	52.34 ± 0.13	0.25	52.31 ± 0.13	0.25
	2	/	/			52.34 ± 0.05	0.09		
	3	/	/			52.40 ± 0.09	0.18		
	4	/	/			52.15 ± 0.08	0.15		

versus non-specific PCR products, and thus, the by-products of the PCR system adversely affect the test performance, greatly limiting its application.

In the present study, we developed a cost-saving method based on asymmetric PCR and a one fluorescent probe-mediated melting curve method to distinguish *UGT1A1**1/*1, *1/*28, and *28/*28, and our analysis showed that the method is accurate and sensitive with outstanding reliability. Our approach represents the first melting curve method combined with asymmetric PCR reported for $(TA)_n$ genotyping that requires only one fluorescent probe. The experimental procedure is simple: asymmetric PCR is used to obtain excess copies of single-stranded amplicons, and the probe is hybridized to the targeted amplicons at low temperature and dissociated as the temperature increases during the melting analysis process. Compared with other methods, the operation requires less time and labor, while the judgment of genotypes is very simple and clear. The probe was designed to perfectly match the *UGT1A1**1 sequence, resulting in a stable double-stranded product and a high T_m when binding to the *1 allele. Meanwhile, the two base pair mismatches caused a 2-bp bulge between the probe and *UGT1A1**28 allele, resulting in a less stable product and a lower T_m. The difference in T_m between the *UGT1A1**1 and *28 peaks is > 4.2°C, which provides good discrimination of the three genotypes. The intra- and inter-assay precision levels were satisfactory at lower than 0.27%, suggesting a better reliability than either the dual-probes melting analysis method[20] or TaqMan real-time PCR method,[33] and the CV for our method was similar to that of the SYBR Green I melting method.[23] Thus, the presented method is able to distinguish the genotypes using the absolute T_m values of the PCR products, and only one *UGT1A1**1/*28 genotype sample is required as a positive control for each run. The method also offers good sensitivity and affords accurate genotyping with an input genomic DNA amount as low as 0.2 ng. Moreover, as a closed-tube PCR assay, the risk of contamination is eliminated in the present method. Therefore, we believe that the method can be well-generalized among different clinical laboratories with good reproducibility when applied using the conditions established in this study.

In addition to genetic testing of *UGT1A1*, a novel methodology to directly measure serum SN-38G and SN-38 will also be helpful to prevent severe adverse effects of irinotecan, as previous studies revealed that the area under the curve (AUC) ratio for SN-38 glucuronide (SN-38G)/SN-38 could be a clinical indicator of irinotecan toxicity and applied for adjustment of the optimal dose. Atasilp et al.[48] developed a technique based on high-performance liquid chromatography (HPLC)/tandem mass spectrometry (MS/MS) that can simultaneously measure the serum concentrations of irinotecan, SN-38, and SN-38G, which may serve as an alternative method to predicting irinotecan toxicity. Studies previously reported that *UGT1A1**28 carriers have high AUC values for irinotecan and SN-38, but a low AUC ratio for SN-38G/SN-38.[49] Thus, we speculated that the combination of detection of irinotecan and its metabolites with genetic testing will allow for more precise use of irinotecan.

In addition to *UGT1A1**28, *UGT1A1**6 (rs4148323), a single nucleotide substitution located in exon 1 that occurs at a relative high frequency in Asians (~20%) can cause an obvious reduction in UGT1A1 enzyme activity and lead to irinotecan-induced diarrhea and neutropenia.[13,14,50–52] Combined genotyping and interpretation of both *UGT1A1**28 and *6 will more fully predict and avoid the adverse effects of irinotecan, especially for Asian populations. Thus, we will further develop a rapid and reliable genotyping method for both *UGT1A1**28 and *6 in the future.

In conclusion, the present method has the following benefits for the discrimination of *UGT1A1**1 and *28 alleles: (a) high accuracy with satisfactory reliability (intra- and inter- run CVs for T_ms were < 0.27%); (b) high sensitivity (limit of detection was 0.2 ng genomic DNA); (c)

simple and labor-saving operation (basically PCR analysis, suitable for both experienced technicians and beginners); (d) avoidance of contamination of PCR products (the melting curve of the amplification product is directly analyzed in a closed-tube); (e) low cost (requiring one fluorescent probe and one positive control for each run); (f) quick operation (the genotype can be identified within 2.5 h); and (g) high-throughput potential in a 96-well or 384-well PCR analyzer. Therefore, we expect this method can be simply and easily generalized for any clinical laboratory with a fluorescent PCR platform.

CONFLICT OF INTEREST

The authors declare that no conflicts of interest exist.

DATA AVAILABILITY STATEMENT

Data available in article supplementary material.

ORCID

Xiaomu Kong https://orcid.org/0000-0002-5920-4759
Peng Gao https://orcid.org/0000-0002-7096-2710

REFERENCES

1. Bosma PJ, Seppen J, Goldhoorn B, et al. Bilirubin UDP-glucuronosyltransferase 1 is the only relevant bilirubin glucuronidating isoform in man. *J Biol Chem*. 1994;269:17960-17964.
2. Bosma PJ, Chowdhury JR, Bakker C, et al. The genetic basis of the reduced expression of bilirubin UDP-glucuronosyltransferase 1 in Gilbert's syndrome. *N Engl J Med*. 1995;333:1171-1175. doi:10.1056/NEJM199511023331802
3. Huang MJ, Lin YC, Liu K, Chang PF, Huang CS. Effects of variation status and enzyme activity for UDP-glucuronosyltransferase 1A1 gene on neonatal hyperbilirubinemia. *Pediatr Neonatol*. 2020;61:506-512. doi:10.1016/j.pedneo.2020.05.009
4. Iyer L, Hall D, Das S, et al. Phenotype-genotype correlation of in vitro SN-38 (active metabolite of irinotecan) and bilirubin glucuronidation in human liver tissue with UGT1A1 promoter polymorphism. *Clin Pharmacol Ther*. 1999;65:576-582. doi:10.1016/S0009-9236(99)70078-0
5. Raijmakers MT, Jansen PL, Steegers EA, Peters WH. Association of human liver bilirubin UDP-glucuronyltransferase activity with a polymorphism in the promoter region of the UGT1A1 gene. *J Hepatol*. 2000;33:348-351. doi:10.1016/s0168-8278(00)80268-8
6. Takano M, Sugiyama T. UGT1A1 polymorphisms in cancer: impact on irinotecan treatment. *Pharmgenomics Pers Med*. 2017;10:61-68. doi:10.2147/PGPM.S108656
7. Beutler E, Gelbart T, Demina A. Racial variability in the UDP-glucuronosyltransferase 1 (UGT1A1) promoter: a balanced polymorphism for regulation of bilirubin metabolism? *Proc Natl Acad Sci USA*. 1998;95:8170-8174. doi:10.1073/pnas.95.14.8170
8. Dean L. *Irinotecan Therapy and UGT1A1 Genotype*. 2012. https://www.ncbi.nlm.nih.gov/pubmed/28520360
9. Burchell B, Hume R. Molecular genetic basis of Gilbert's syndrome. *J Gastroenterol Hepatol*. 1999;14:960-966. doi:10.1046/j.1440-1746.1999.01984.x
10. Iyer L, Das S, Janisch L, et al. UGT1A1*28 polymorphism as a determinant of irinotecan disposition and toxicity. *Pharmacogenomics J*. 2002;2:43-47. doi:10.1038/sj.tpj.6500072
11. Atasilp C, Chansriwong P, Sirachainan E, et al. Effect of drug metabolizing enzymes and transporters in Thai colorectal cancer patients treated with irinotecan-based chemotherapy. *Sci Rep*. 2020;10:13486. doi:10.1038/s41598-020-70351-0
12. Kimura K, Yamano T, Igeta M, et al. UGT1A1 polymorphisms in rectal cancer associated with the efficacy and toxicity of preoperative chemoradiotherapy using irinotecan. *Cancer Sci*. 2018;109:3934-3942. doi:10.1111/cas.13807
13. Ma X, Han S, Liu Y, Liu JT, Fang J, Zhang YH. Pharmacogenetic impact of UGT1A1 polymorphisms on pulmonary neuroendocrine tumours treated with metronomic irinotecan-based chemotherapy in Chinese populations. *J Pharm Pharmacol*. 2020;72:1528-1535. doi:10.1111/jphp.13333
14. Chen S, Hua L, Feng C, et al. Correlation between UGT1A1 gene polymorphism and irinotecan chemotherapy in metastatic colorectal cancer: a study from Guangxi Zhuang. *BMC Gastroenterol*. 2020;20:96. doi:10.1186/s12876-020-01227-w
15. Gil J, Sasiadek MM. Gilbert syndrome: the UGT1A1*28 promoter polymorphism as a biomarker of multifactorial diseases and drug metabolism. *Biomark Med*. 2012;6:223-230. doi:10.2217/BMM.12.4
16. Hu ZY, Yu Q, Pei Q, Guo C. Dose-dependent association between UGT1A1*28 genotype and irinotecan-induced neutropenia: low doses also increase risk. *Clin Cancer Res*. 2010;16:3832-3842. doi:10.1158/1078-0432.CCR-10-1122
17. Liu XH, Lu J, Duan W, et al. Predictive value of UGT1A1*28 polymorphism in Irinotecan-based chemotherapy. *J Cancer*. 2017;8:691-703. doi:10.7150/jca.17210
18. Gurtler V, Parkin JD, Mayall BC. Use of double gradient denaturing gradient gel electrophoresis to detect (AT)n polymorphisms in the UDP-glucuronosyltransferase 1 gene promoter associated with Gilbert's syndrome. *Electrophoresis*. 1999;20:2841-2843. doi:10.1002/(SICI)1522-2683(19991001)20:14<2841::AID-ELPS2841>3.0.CO;2-V
19. Borlak J, Thum T, Landt O, Erb K, Hermann R. Molecular diagnosis of a familial nonhemolytic hyperbilirubinemia (Gilbert's syndrome) in healthy subjects. *Hepatology*. 2000;32:792-795. doi:10.1053/jhep.2000.18193
20. von Ahsen N, Oellerich M, Schutz E. DNA base bulge vs unmatched end formation in probe-based diagnostic insertion/deletion genotyping: genotyping the UGT1A1 (TA) (n) polymorphism by real-time fluorescence PCR. *Clin Chem*. 2000;46:1939-1945.
21. Hsieh TY, Shiu TY, Chu NF, et al. Rapid molecular diagnosis of the Gilbert's syndrome-associated exon 1 mutation within the UGT1A1 gene. *Genet Mol Res*. 2014;13:670-679. doi:10.4238/2014.January.28.12
22. Ishige T, Itoga S, Kawasaki K, et al. Multiplex PCR and multicolor probes melting for the simultaneous detection of five UGT1A1 variants. *Anal Biochem*. 2019;587:113448. doi:10.1016/j.ab.2019.113448
23. Marziliano N, Pelo E, Minuti B, Passerini I, Torricelli F, Da Prato L. Melting temperature assay for a UGT1A gene variant in Gilbert syndrome. *Clin Chem*. 2000;46:423-425.
24. Arambula E, Vaca G. Genotyping by "cold single-strand conformation polymorphism" of the UGT1A1 promoter polymorphism in Mexican mestizos. *Blood Cells Mol Dis*. 2002;28:86-90. doi:10.1006/bcmd.2001.0481
25. Saeki M, Saito Y, Jinno H, et al. Comprehensive UGT1A1 genotyping in a Japanese population by pyrosequencing. *Clin Chem*. 2003;49:1182-1185. doi:10.1373/49.7.1182
26. Skarke C, Grosch S, Geisslinger G, Lotsch J. Single-step identification of all length polymorphisms in the UGT1A1 gene promoter. *Int J Clin Pharmacol Ther*. 2004;42:133-138. doi:10.5414/cpp42133
27. Sukasem C, Atasilp C, Chansriwong P, Chamnanphon M, Puangpetch A, Sirachainan E. Development of pyrosequencing method for detection of UGT1A1 polymorphisms in Thai colorectal cancers. *J Clin Lab Anal*. 2016;30:84-89. doi:10.1002/jcla.21820
28. Hasegawa Y, Sarashina T, Ando M, et al. Rapid detection of UGT1A1 gene polymorphisms by newly developed invader assay. *Clin Chem*. 2004;50:1479-1480. doi:10.1373/clinchem.2004.034694

29. Huang CK, Dulau A, Su-Rick CJ, Pan Q. Validation of rapid polymerase chain reaction-based detection of all length polymorphisms in the UGT 1A1 gene promoter. *Diagn Mol Pathol*. 2007;16:50-53. doi:10.1097/01.pdm.0000213467.91139.c9
30. Jiraskova A, Lenicek M, Vitek L. Simultaneous genotyping of microsatellite variations in HMOX1 and UGT1A1 genes using multicolored capillary electrophoresis. *Clin Biochem*. 2010;43:697-699. doi:10.1016/j.clinbiochem.2010.01.006
31. Abou Tayoun AN, de Abreu FB, Lefferts JA, Tsongalis GJ. A clinical PCR fragment analysis assay for TA repeat sizing in the UGT1A1 promoter region. *Clin Chim Acta*. 2013;422:1-4. doi:10.1016/j.cca.2013.03.023
32. Ehmer U, Lankisch TO, Erichsen TJ, et al. Rapid allelic discrimination by TaqMan PCR for the detection of the Gilbert's syndrome marker UGT1A1*28. *J Mol Diagn*. 2008;10:549-552. doi:10.2353/jmoldx.2008.080036
33. Dapra V, Alliaudi C, Galliano I, et al. TaqMan real time PCR for the detection of the Gilbert's syndrome markers UGT1A1*28; UGT1A1*36 and UGT1A1*37. *Mol Biol Rep*. 2021;48:4953-4959. doi:10.1007/s11033-021-06454-2
34. Minucci A, Concolino P, Giardina B, Zuppi C, Capoluongo E. Rapid UGT1A1 (TA) (n) genotyping by high resolution melting curve analysis for Gilbert's syndrome diagnosis. *Clin Chim Acta*. 2010;411:246-249. doi:10.1016/j.cca.2009.11.013
35. Farrar JS, Palais RA, Wittwer CT. Snapback primer genotyping of the Gilbert syndrome UGT1A1 (TA) (n) promoter polymorphism by high-resolution melting. *Clin Chem*. 2011;57:1303-1310. doi:10.1373/clinchem.2011.166306
36. Mlakar SJ, Ostanek B. Development of a new DHPLC assay for genotyping UGT1A (TA)n polymorphism associated with Gilbert's syndrome. *Biochem Med (Zagreb)*. 2011;21:167-173. doi:10.11613/bm.2011.026
37. Fesenko EE, Heydarov RN, Stepanova EV, et al. Microarray with LNA-probes for genotyping of polymorphic variants of Gilbert's syndrome gene UGT1A1(TA)n. *Clin Chem Lab Med*. 2013;51:1177-1184. doi:10.1515/cclm-2012-0656
38. Shiu TY, Huang HH, Lin HH, et al. Restriction fragment length polymorphism effectively identifies exon 1 mutation of UGT1A1 gene in patients with Gilbert's syndrome. *Liver Int*. 2015;35:2050-2056. doi:10.1111/liv.12785
39. Song J, Sun M, Li J, Zhou D, Wu X. Three-dimensional polyacrylamide gel-based DNA microarray method effectively identifies UDP-glucuronosyltransferase 1A1 gene polymorphisms for the correct diagnosis of Gilbert's syndrome. *Int J Mol Med*. 2016;37:575-580. doi:10.3892/ijmm.2016.2453
40. Baudhuin LM, Highsmith WE, Skierka J, Holtegaard L, Moore BE, O'Kane DJ. Comparison of three methods for genotyping the UGT1A1 (TA)n repeat polymorphism. *Clin Biochem*. 2007;40:710-717. doi:10.1016/j.clinbiochem.2007.03.007
41. Sissung TM, Barbier RH, Price DK, et al. Comparison of eight technologies to determine genotype at the UGT1A1 (TA)n repeat polymorphism: potential clinical consequences of genotyping errors? *Int J Mol Sci*. 2020;21:896. doi:10.3390/ijms21030896
42. Zhu J, Liu A, Sun X, et al. Multicenter, randomized, phase III trial of neoadjuvant chemoradiation with capecitabine and Irinotecan guided by UGT1A1 status in patients with locally advanced rectal cancer. *J Clin Oncol*. 2020;38:4231-4239. doi:10.1200/JCO.20.01932
43. Tsai HL, Huang CW, Lin YW, et al. Determination of the UGT1A1 polymorphism as guidance for irinotecan dose escalation in metastatic colorectal cancer treated with first-line bevacizumab and FOLFIRI (PURE FIST). *Eur J Cancer*. 2020;138:19-29. doi:10.1016/j.ejca.2020.05.031
44. Paez D, Tobena M, Fernandez-Plana J, et al. Pharmacogenetic clinical randomised phase II trial to evaluate the efficacy and safety of FOLFIRI with high-dose irinotecan (HD-FOLFIRI) in metastatic colorectal cancer patients according to their UGT1A 1 genotype. *Br J Cancer*. 2019;120:190-195. doi:10.1038/s41416-018-0348-7
45. Fujii H, Yamada Y, Watanabe D, et al. Dose adjustment of irinotecan based on UGT1A1 polymorphisms in patients with colorectal cancer. *Cancer Chemother Pharmacol*. 2019;83:123-129. doi:10.1007/s00280-018-3711-8
46. Hulshof EC, Deenen MJ, Guchelaar HJ, Gelderblom H. Pretherapeutic UGT1A1 genotyping to reduce the risk of irinotecan-induced severe toxicity: ready for prime time. *Eur J Cancer*. 2020;141:9-20. doi:10.1016/j.ejca.2020.09.007
47. Haberl M, Tautz D. Comparative allele sizing can produce inaccurate allele size differences for microsatellites. *Mol Ecol*. 1999;8:1347-1349. doi:10.1046/j.1365-294x.1999.00692_1.x
48. Atasilp C, Chansriwong P, Sirachainan E, et al. Determination of irinotecan, SN-38 and SN-38 glucuronide using HPLC/MS/MS: application in a clinical pharmacokinetic and personalized medicine in colorectal cancer patients. *J Clin Lab Anal*. 2018;32:e22217. doi:10.1002/jcla.22217
49. Wang Y, Shen L, Xu N, et al. UGT1A1 predicts outcome in colorectal cancer treated with irinotecan and fluorouracil. *World J Gastroenterol*. 2012;18:6635-6644. doi:10.3748/wjg.v18.i45.6635
50. Atasilp C, Chansriwong P, Sirachainan E, et al. Correlation of UGT1A1(*)28 and (*)6 polymorphisms with irinotecan-induced neutropenia in Thai colorectal cancer patients. *Drug Metab Pharmacokinet*. 2016;31:90-94. doi:10.1016/j.dmpk.2015.12.004
51. Hikino K, Ozeki T, Koido M, et al. Comparison of effects of UGT1A1*6 and UGT1A1*28 on irinotecan-induced adverse reactions in the Japanese population: analysis of the biobank Japan project. *J Hum Genet*. 2019;64:1195-1202. doi:10.1038/s10038-019-0677-2
52. Zhu X, Ma R, Ma X, Yang G. Association of UGT1A1*6 polymorphism with irinotecan-based chemotherapy reaction in colorectal cancer patients: a systematic review and a meta-analysis. *Biosci Rep*. 2020;40:BSR20200576. doi:10.1042/BSR20200576

SUPPORTING INFORMATION

Additional supporting information can be found online in the Supporting Information section at the end of this article.

How to cite this article: Kong X, Xu Y, Gao P, et al. Rapid detection of the irinotecan-related *UGT1A1*28* polymorphism by asymmetric PCR melting curve analysis using one fluorescent probe. *J Clin Lab Anal*. 2022;36:e24578. doi: 10.1002/jcla.24578